Progress In Electromagnetics Research M, Vol. 50, 55–63, 2016

Numerical Simulations of ELF/VLF Wave Generated by Modulated Beat-Wave Ionospheric Heating in High Latitude Regions

Haiying Li[1, 2, *], Jie Zhan[1], Zhensen Wu[1, 2], and Pengfei Kong[1]

Abstract—Based on the theory of ionospheric heating, with the self-consistent model in the low ionosphere, the Extremely-Low-Frequency (ELF) and Very-Low-Frequency (VLF) waves generated by modulated beat-wave ionospheric heating are analyzed theoretically. In the consideration of the stratified ionosphere, the magnetic fields generated by the equivalent ELF/VLF dipole source above the sea surface are studied by using the quasi-longitudinal approximation method. Taking the high latitude regions as an example, the variations of the electron temperature, the increments of Pedersen and Hall conductivities and the changing of the oscillating current density with the modulation frequency in beat-wave heating are numerically discussed. The distribution of the magnetic fields is presented. It turns out that in high latitude regions, the efficiency of rectangular wave modulated heating in generating ELF/VLF wave is higher than that of modulated beat-wave heating, and the order of magnitude of the magnetic fields received above the sea surface is 10^{-7} A/m in beat-wave modulation.

1. INTRODUCTION

Extremely-Low-Frequency (ELF) and Very-Low-Frequency (VLF) waves have characteristics of long wavelength, low loss in propagation path, stable phase and magnitude. Natural electric fields in low ionosphere provide an important advantage for the form of equivalent ELF/VLF antenna by period modulation of HF (high frequency) heating technique. Compared with the traditional ground ELF/VLF antenna, this kind of antenna has the characteristics of higher sensitive, smaller size, higher hiding and smaller pollution. Study on the ELF/VLF waves generated by modulated heating technique and ELF/VLF wave propagation in Earth-ionosphere waveguide plays an important role in the fields of under-ground objects detection [1], underwater communications [2] and earthquake prediction [3].

For the ELF/VLF wave generation in low ionosphere, the methods of modulated HF heating and the effects of heating parameters on radiation efficiency are widely studied from both the experimental and theoretical points. Using the ionospheric heaters of High Frequency Active Auroral Research Program (HAARP), several modulated heating experiments were carried out, and properties of ELF/VLF waves generated by electrojet modulation were presented, such as the azimuth, polarization, frequency dependence [4], and ELF/VLF perturbations by the DEMETER satellite [5]. Except rectangular wave modulation, the beat-wave heating technique [6] is one typical method to generate ELF/VLF waves. Kuo [7] presented the magnitudes of ELF/VLF signals in both day and night during the beat-wave heating experiments. Moore [8] carried out the beat-wave heating in different environments, and studied the site of ELF/VLF sources by T-O-A (Time-of-arrival) method. Barr and Stubbe [9] pointed out that beat-wave heating technique depended on heating equipments with higher power. Taking advantage of EISCAT's (Europe Incoherent Scatter Scientific Association) heating facility, some beat-wave experiments were also launched. For example, Fedorenko [10] gave the influences of Earth-ionosphere waveguide on the polarization of ELF/VLF waves, Tereshchenko [11] presented the

Received 26 June 2016, Accepted 3 September 2016, Scheduled 16 September 2016
* Corresponding author: Haiying Li (lihy@xidian.edu.cn).
[1] School of Physics and Optoelectronic Engineering, Xidian University, Xi'an 710071, China. [2] Collaborative Innovation Center of Information Sensing and Understand at Xidian University, Xi'an 710071, China.

features of amplitude and Doppler frequency variation of ELF/VLF waves, and Gavrilov [12] analyzed the amplitude-phase characteristics of ELF/VLF waves by the measurement results. Although many observations of beating-wave experiments and their analysis have been carried out by both HAARP and EISCAT's facilities, for the purpose of comparative analysis, the mechanism of beat-wave heating method still needs an intensive study, such as the theoretical simulation of the conductivities, and the oscillating current density. It is just the main issue of this research.

Since 1960, many scholars began to study the propagation of ELF/VLF in ionosphere and Earth-ionosphere waveguide [13, 14]. In 2004, Pan [15] thoroughly discussed the theoretical calculation method of the propagation of ELF/VLF waves in ionosphere and Earth-ionosphere waveguide. As an important method of solving the propagation of ELF/VLF waves, Fourier transform method was used to solve the magnetic fields above sea surface caused by equivalent ELF/VLF dipole sources of ionospheric heating [16]. The ray tracing method was also used to discuss the propagation of ELF/VLF waves [17]. So as to calculate the magnetic fields radiated from the equivalent dipole sources of beat-wave heating in high latitude regions, quasi-longitudinal approximation of Fourier transform method is chosen in this paper.

In this work, based on the self-consistent heating model in low ionosphere, considering the beat-wave heating in high latitude regions, the variations of conductivities and oscillating currents with heating periods and modulating frequencies are calculated and discussed in detail. Due to the changing of electron density and collision frequency with ionospheric altitudes, suppose that the ionosphere is stratified, and with the quasi-longitudinal approximation method, the distribution of magnetic fields above the sea surface which are radiated by the equivalent dipole sources in beat-wave heating process is presented.

2. BASIC THEORY

2.1. Beat-Wave Heating Model in Low Ionosphere

Ohmic heating effects are predominant in low ionosphere. The self-consistent heating model [18] provides a way to describe the ohmic heating process, and can be given by:

$$\frac{3}{2}n_{\mathrm{e}}k_{\mathrm{B}}\frac{\mathrm{d}T_{\mathrm{e}}}{\mathrm{d}t} = 2k\chi S - L_{\mathrm{e}}\left(T_{\mathrm{e}}, T_0\right) \tag{1}$$

Equation (1) denotes the variation of electron temperature with heating period, where T_{e} is the electron temperature, n_{e} the electron density, k_{B} the Boltzmann constant, k the absorption index, χ the imaginary of A-H refractive index, S the energy density of HF heating wave, and L_{e} the total loss of electron energy.

The formula of A-H refractive index is:

$$n^2 = (\gamma + \mathrm{i}\chi)^2 = 1 - 2X\frac{1 - \mathrm{i}Z - X}{2(1 - \mathrm{i}Z)(1 - \mathrm{i}Z - X) - Y_{\mathrm{T}}^2 \pm \sqrt{Y_{\mathrm{T}}^2 + 4Y_{\mathrm{L}}^2(1 - \mathrm{i}Z - X)^2}} \tag{2}$$

In Equation (2), $X = f_{\mathrm{N}}^2/f^2$, $Y = f_{\mathrm{H}}/f^2$, $Z = v_{\mathrm{en}}/2\pi f$, f is the frequency of HF heating wave, $f_{\mathrm{N}} = \sqrt{n_{\mathrm{e}}\mathrm{e}^2/4\pi^2\varepsilon_0 m}$ is the plasma frequency, $f_{\mathrm{H}} = \mathrm{e}B/2\pi m$ is the electron gyro-frequency, and B is calculated by the center dipole geomagnetic field model. $Y_{\mathrm{T}} = Y\sin\varphi$, $Y_{\mathrm{L}} = Y\cos\varphi$, φ is the angle between normal of incident wave and geomagnetic field, $\pm$ represents the O and X modes respectively, and v_{en} is the collision frequency between electrons and neutral particles.

Due to the absorption index $k = \omega\chi/c$, the incident energy flux is:

$$S(h) = \frac{P_{\mathrm{E}}}{4\pi h^2}\exp\left[-2\int_{h_1}^{h} k(h')\mathrm{d}h'\right] \tag{3}$$

where P_{E} is the effective radiated power (ERP), c the velocity of light, and ω the angular frequency of the HF heating wave.

Two HF antenna subarrays are used in the beat-wave heating experiments. The schema of beat-wave modulated heating is shown in Figure 1.

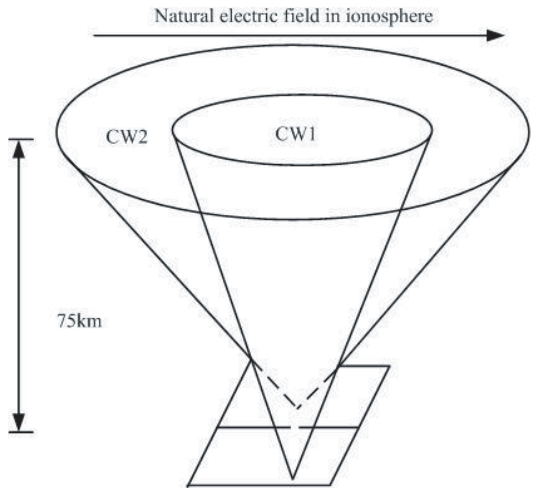

Figure 1. Beat-wave modulated heating model.

Because the frequencies of HF heating waves are much bigger than that of the ELF/VLF wave, the superposition of two continue waves is beat-wave. In the process of beat-wave heating, the frequency difference of the two continue waves radiated from antenna subarrays will modulate the electrical conductivity of D region efficiently. With the relationship between the conductivity increment and the natural electric field E_0, the oscillating current density can be written as:

$$\delta J_S = \Delta\sigma E_0 \tag{4}$$

The frequency difference is just the frequency of ELF/VLF wave. The oscillating current can be equivalent to a dipole source, and the dipole moment of the equivalent ELF/VLF antenna can also be calculated.

3. MAGNETIC FIELDS ABOVE SEA SURFACE BY QUASI-LONGITUDINAL APPROXIMATION METHOD

In high latitude regions, the dipole source generated by the beat-wave modulation can be equivalent to an ELF/VLF transmit antenna. The ELF/VLF waves will propagate through ionosphere, troposphere and stratosphere and arrive at the receiving position finally.

The equivalent physical model in Figure 2 is used. Suppose that the geomagnetic field B is in the x-z plane and that the angle between z and B is φ. Because angle φ is very small in high latitude regions, the ELF/VLF antenna can be equivalent to a horizontal dipole. The radiation source, which is the equivalent dipole antenna, is placed in the D region of ionosphere. The wave from the radiation source is first through the D region. Variations of ionosphere plasma within one wavelength range of ELF/VLF wave are very large, and this inhomogeneity will influence the propagation characteristics of ELF/VLF waves. Therefore, the ionospheric plasma in D region is seen as an n-layer medium. Then, the wave enters the Earth-ionosphere waveguide and is finally received by the facility above the ground or sea surface.

With the Fourier transformation and quasi-longitudinal approximation method, the field expressions above sea surface generated by the dipole source in the layered ionosphere can be obtained. The magnetic fields can be shown as [19]:

$$H_\rho = \frac{IdlQ}{2k_0\pi\eta}\mathrm{e}^{\mathrm{i}k_0\lambda_1(d_1-z_0)}\exp\left(-\mathrm{i}k_0\int_{z_0}^{z_1}\lambda_1\mathrm{d}z\right)\mathrm{e}^{\mathrm{i}\,\mathrm{sign}(n_b)\varphi}\sum_{j=0}^{\infty}\mathrm{e}^{\mathrm{i}k_0R_j}\left[\frac{2}{R_j^3}-\frac{\mathrm{i}2k_0}{R_j^2}-\left(\frac{(2j+1)d_1}{R_j}\right)^2\left(\frac{3}{R_j^3}-\frac{\mathrm{i}3k_0}{R_j^2}-\frac{k_0^2}{R_j}\right)\right] \tag{5}$$

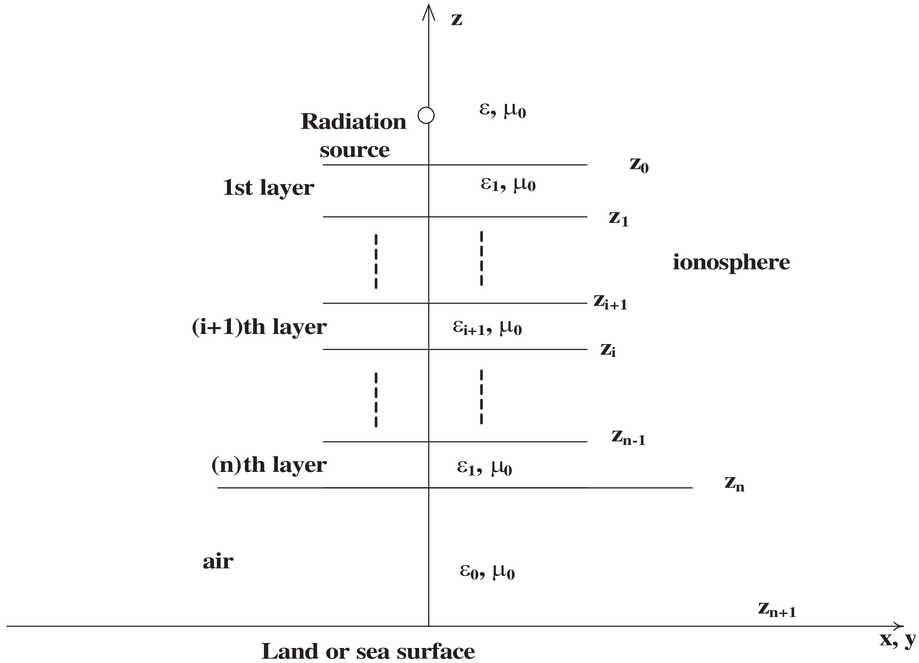

Figure 2. ELF/VLF wave propagation path physical model.

$$H_\varphi = \frac{\mathrm{i}IdlQ}{2k_0\pi\eta}\mathrm{e}^{\mathrm{i}k_0\lambda_1(d_1-z_0)}\exp\left(-\mathrm{i}k_0\int_{z_0}^{z_1}\lambda_1\mathrm{d}z\right)\mathrm{e}^{\mathrm{i}\,\mathrm{sign}(n_b)\varphi}\sum_{j=0}^{\infty}\mathrm{e}^{\mathrm{i}k_0R_j}\left(-\frac{1}{R_j^3}+\frac{\mathrm{i}k_0}{R_j^2}+\frac{k_0^2}{R_j}\right) \tag{6}$$

where $Q = L_{11}\sin k_0z_n/2P_0$, $R_j = [(2j+1)^2d_1^2+\rho^2]^{1/2}$, $P_0 = \sqrt{|n_b|\,\omega_H\omega_0/\omega_p^2}$, ω_H is the electron cyclotron frequency, ω_p the electron plasma frequency, and n_b the z direction of geomagnetic field. $\mathrm{sign}(n_b)$ represents $n_b/|n_b|$. $\eta = \sqrt{\mu_0/\varepsilon_0}$ is the wave impedance in free space, I the current generated by beating-wave heating, L_{11} the horizontal scale of dipole moment, and d_1 the lowest boundary of ionosphere.

4. NUMERICAL RESULTS ANALYSIS AND DISCUSSION

In this section, the characteristics of beat-wave heating experiments in high latitude regions are simulated in detail. The frequencies of the two continue waves are $f_1 = 4.1\,\mathrm{MHz}$ and $f_2 = f_1 + 1000\,\mathrm{Hz}$, respectively. The effective radiation power is 1.16 GW. The heating wave is X mode. The heating site is Tromsø. The time is at 12 : 00 (Local Time) on 20 November 2014. With Equation (1), Figures 3(a)–(d) show the oscillation variations of electron temperature with heating time at 75 km, 80 km, 85 km and 90 km.

It is indicated from Figure 3 that the variation of electron temperature with heating time is a periodic oscillation, and the period is equal to the frequency difference. It is evident that the electron temperature is well modulated in the altitude range 60 km–90 km. Comparing Figure 3(a) with Figure 3(d), once the heater is on, the electron temperature at 75 km reaches a steady state quickly, however, it needs a long time before the electron temperature at 90 km becomes periodic oscillation. The reason is that the period of beat-wave is larger than the time constant at 75 km whereas this is just converse at 90 km, and therefore, the heating process will reach steadiness swiftly. As the altitude increases, the maximum of electron temperature decreases gradually, and the range of oscillation magnitude also decreases.

In order to reflect the changing of electron temperature with ionospheric altitudes at different heating times intuitively, the variations of electron temperature in one period are given by Figure 4.

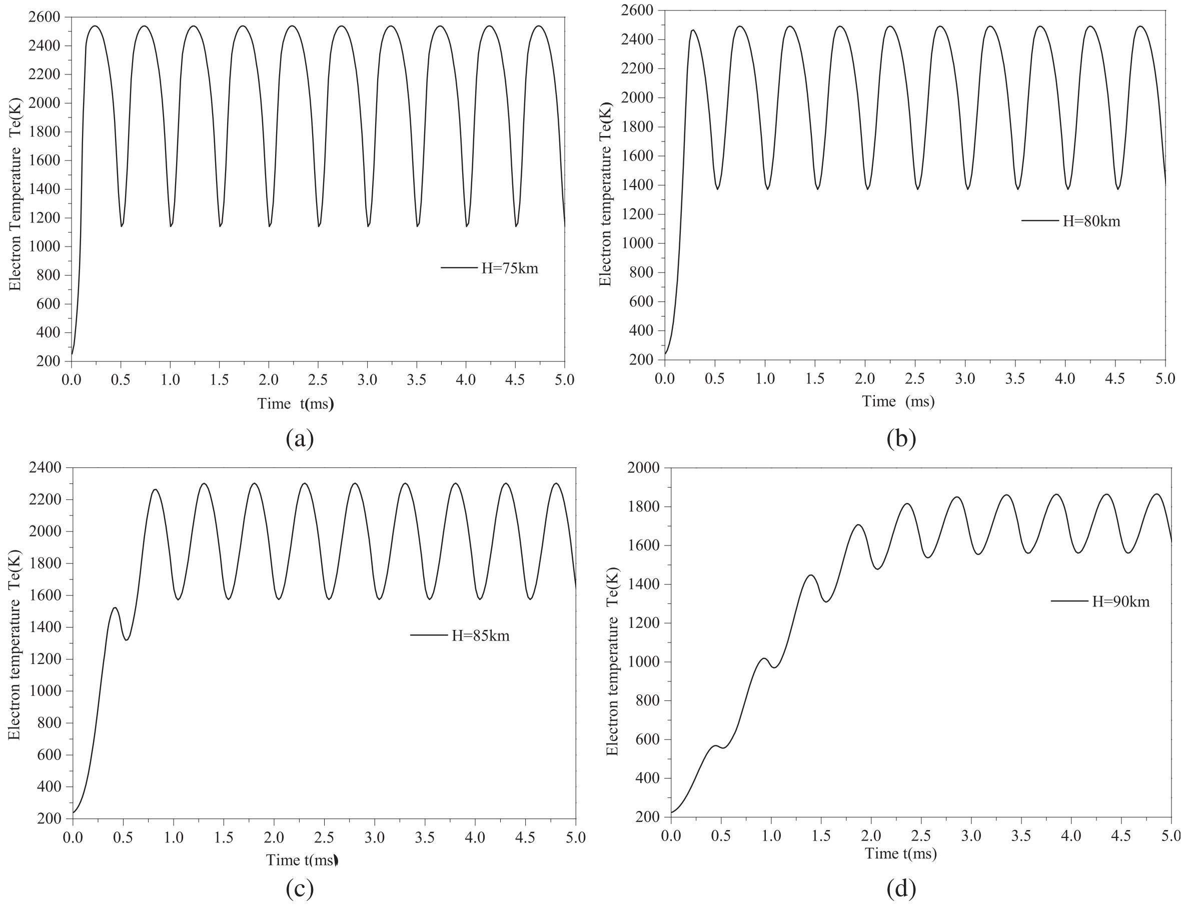

Figure 3. Variations of electron temperature with heating time at different altitudes.

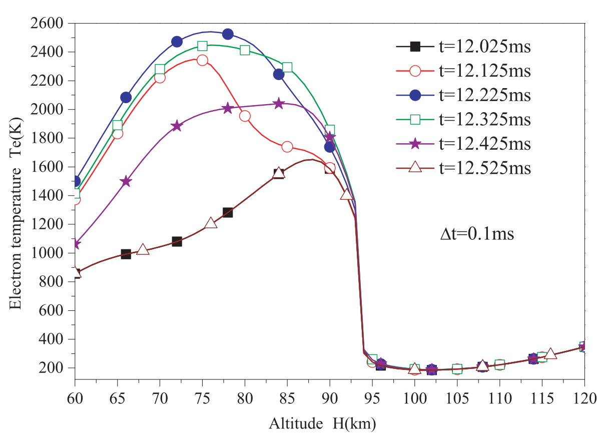

Figure 4. Variations of electron temperature with different heating moments in one period.

Figure 4 reveals that the electron temperature firstly reaches the maximum and then decreases to the undisturbed value gradually in one beat-wave period. Within 0.1 ms of the heating period, the electron temperature below 75 km will arrive at the steady state rapidly. While the altitude is around 90 km, the electron temperature is basically unvarying. Large change of electron temperature is in the altitude range 60 km–85 km. When the altitude reaches 90 km, the variations are no longer apparent.

As well known, under the influence of the ionospheric electric field, the current density in ionosphere can be written as:

$$\vec{J} = \sigma_{//}\vec{E}_{//} + \sigma_p\vec{E}_\perp + \sigma_H\left(\vec{b} \times \vec{E}\right) = \overline{\overline{\sigma}} \cdot \vec{E}_0 \tag{7}$$

where $\sigma_{//}$, σ_P and σ_H denote parallel, Pedersen and Hall conductivities, respectively. They are given by:

$$\sigma_{//} = \frac{n_e e}{B}\left(\frac{\omega_e}{v_{en}} + \frac{\omega_i}{v_{in}}\right) \tag{8}$$

$$\sigma_p = \frac{en_e}{B}\left(\frac{\omega_e v_{en}}{v_{en}^2 + \omega_e^2} + \frac{\omega_i v_{in}}{v_{in}^2 + \omega_i^2}\right) \tag{9}$$

$$\sigma_H = \frac{en_e}{B}\left(\frac{\omega_e^2}{v_{en}^2 + \omega_e^2} - \frac{\omega_i^2}{v_{in}^2 + \omega_i^2}\right) \tag{10}$$

When the electron temperature is modulated by beat-wave, the collision frequency v_{en} between electrons and neutral particles will also be modulated with the same frequency. Substituting the modulated collision frequency v_{en} into the above expressions, the variations of conductivities in beat-wave heating process can be obtained directly. Pedersen and Hall conductivity variations $\Delta\sigma_\mathrm{P}$, $\Delta\sigma_\mathrm{H}$ in one heating period are given in Figure 5.

It is obvious that there are two peaks in Figure 5(a) and Figure 5(b). The first one, which is in the altitude range 60 km–85 km, is caused by the increasing of electron temperature, and the other, which is in the altitude range 90 km–95 km, is aroused by the increase of electron density. In Figure 5(a), the jumping phase near 77 km cancels out part of Pedersen currents; therefore, the Pedersen currents decrease, and this result is similar to the conclusion in reference [20].

Through solving the integral of oscillating current density over ionosphere altitudes, the variations of oscillating current magnitude with modulating frequencies are shown in Figure 6. It turns out that in the frequency range 1 KHz–10 KHz, oscillating currents generated by beat-wave modulation are smaller than those of rectangular wave modulation. As the modulating frequencies increase, the oscillating current magnitudes decrease.The experimental results provided by Barr and Stubbe [21] pointed out that for the frequencies 565 Hz and 2005 Hz, the signal of rectangular wave modulation was larger than that of beat-wave modulation by about 11 dB. The results in Figure 6 verify this point exactly. Making use of the modulating signal quality analysis method [22], it leads to the efficiency of beat-wave modulation smaller than that of rectangular wave in the same condition, but the signal quality of beat-wave is the best. Because there is no high harmonics in signals of beat-wave modulation. With the HAARP's heating facility, Cohen et al. [23] verified this conclusion.

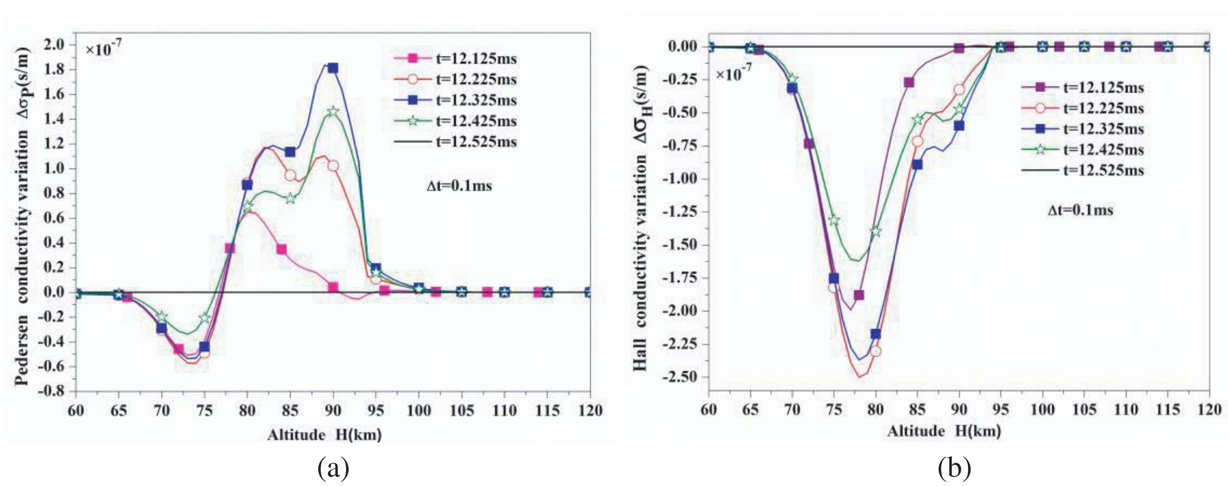

Figure 5. Altitude profile of conductivity variations $\Delta\sigma_\mathrm{P}$ and $\Delta\sigma_\mathrm{H}$. (a) Pedersen conductivity variations. (b) Hall conductivity variations.

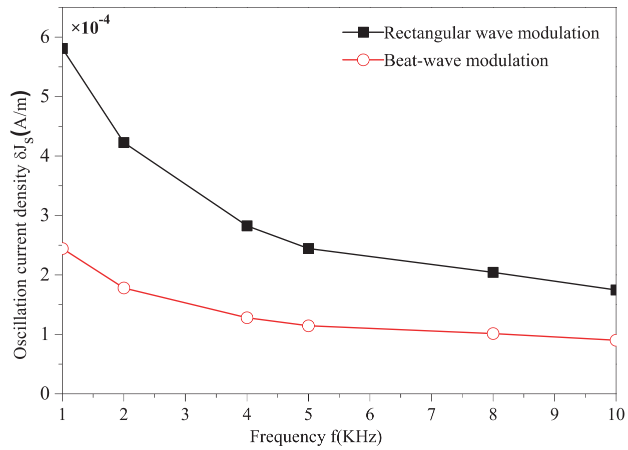

Figure 6. Oscillating current magnitudes of both rectangular wave and beat-wave modulated heating.

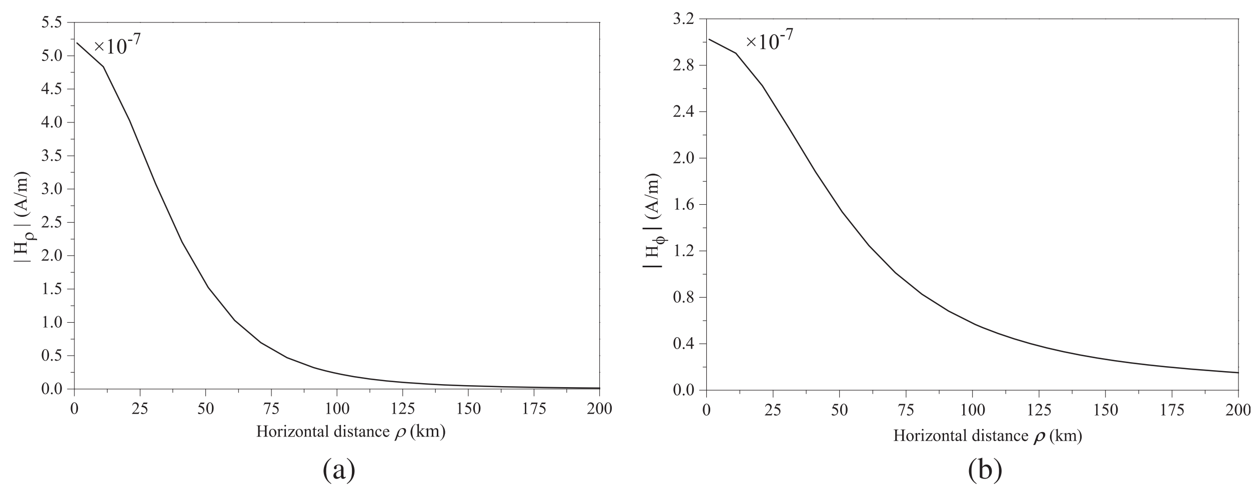

Figure 7. Magnitudes of magnetic fields above sea surface caused by beat-wave heating in low ionosphere. (a) ρ axis. (b) ϕ axis.

From Figure 6, when the frequency of VLF wave is 1 KHz, the integrality of oscillating current density is 2.445×10^{-4} A/m. The position of dipole source is located at the altitude of Hall conductivity maximum, which is about 78 km from Figure 5. Reference [6] reveals that the distance L of modulating region is about 20 km. Using these parameters, the dipole moment of horizontal dipole generated by beat-wave modulation is $97.8\,\mathrm{A} \cdot \mathrm{km}$.

By the quasi-longitudinal approximation method, the variations of magnetic field magnitude with propagation distances are given in Figure 7. The order of magnitudes is about 10^{-7} A/m, and this signal can be received. Magnitudes of the magnetic field decrease gradually with the increasing propagation distances. Within the distance 80 km, the magnitudes fall off rapidly. Compared with the results of rectangular wave modulation in reference [24], the magnetic field magnitudes of beat-wave modulation are smaller. There are two reasons for the decrease of magnetic field magnitudes. One is that the dipole moment of beat-wave modulation is smaller than that of rectangular wave modulation, and the other is that the ionosphere region from 60 km–78 km is considered as inhomogeneous plasma in our simulation. The conclusion in [19] shows that the magnetic field magnitudes for the inhomogeneous ionosphere are smaller than those for the homogeneous ionosphere.

5. CONCLUSIONS

On the basis of self-consistent ionospheric heating model and quasi-longitudinal approximation of Fourier transformation method, simulation of ELF/VLF waves generated by beat-wave heating and their downward propagation are studied. The discussion of variation of electron temperature, conductivities, oscillating currents and magnetic field magnitude is given. A comparison of our results with previous work is also presented. Several conclusions can be obtained. The electron temperature is well modulated in the altitude range 60 km–90 km. Oscillating currents generated by beat-wave modulation are smaller than those of rectangular wave modulation. The order of magnetic field magnitudes caused by beat-wave heating above sea surface is 10^{-7} A/m, and the magnetic field magnitudes are smaller than those of rectangular wave heating. Results in this paper may provide theoretical basis for the improvement of ELF/VLF wave generation efficiency by ionospheric heating technique.

ACKNOWLEDGMENT

This work was supported by National Natural Science Foundation of China (Nos. 61475123, 61571355) and The Project Supported by Natural Science Basic Research Plan in Shaanxi Province of China (No. 2016JQ4015).

REFERENCES

1. Stolarczyk, L. G., "Detection and imaging of underground structures by exploiting ELF/VLF radiowaves," AFRL-VS-TR-2000-1583, 2000.
2. Doniec, M., M. Angermann, and D. Rus, "An end-to-end signal strength model for underwater optical communications," *IEEE Journal of Oceanic Engineering*, Vol. 38, 743–757, 2013.
3. Wang, Y.-X., R.-H. Jin, X.-L. Liang, and J.-P. Geng, "Propagation of SLF/ELF electromagnetic waves excited by an underground HED in the lower ionosphere," *IEEE Transactions on Antennas and Propagation*, Vol. 60, No. 11, 5412–5418, 2012.
4. Maxworth, A. S., M. Golkowski, M. B. Cohen, et al., "Multistation observations of the azimuth, polarization, and frequency dependence of ELF/VLF waves generated by electrojet modulation," *Radio Science*, Vol. 50, 1008–1026, 2015.
5. Titova, E. E., A. G. Demekhov, A. A. Mochalov, et al., "ELF/VLF perturbations above the HAARP transmitter recorded by the Demeter satellite in the upper ionosphere," *Radiophysics and Quantum Electronics*, Vol. 58, 155–172, 2015.
6. Papadopoulos, K., C. L. Chang, P. Vitello, et al., "On the efficiency of ionospheric ELF generation," *Radio Science*, Vol. 25, 1311–1320, 1990.
7. Kuo, S., A. Snyder, P. Kossey, et al., "Beating HF waves to generate VLF waves in the ionosphere," *Journal of Geophysical Research Space Physics*, Vol. 117, 1–83, 2012.
8. Moore, R. C., S. Fujimaru, M. Cohen, et al., "On the altitude of the ELF/VLF source region generated during "beat-wave" HF heating experiments," *Geophysical Research Letters*, Vol. 39, No. 18, L18101, 2012.
9. Barr, R. and P. Stubbe, "On the ELF generation efficiency of the Tromsø Heater Facility," *Geophysical Research Letters*, Vol. 18, 1971–1974, 1991.
10. Fedorenko, Yu, E. O. Tereshchenko, S. Pilgaev, et al., "Polarization of ELF waves generated during "beat-wave" heating experiment near cutoff frequency of the Earth-ionosphere waveguide," *Radio Science*, Vol. 49, 1254–1264, 2014.
11. Tereshchenko, E. O., O. I. Shumilov, E. A. Kasatkina, et al., "Features of amplitude and Doppler frequency variation of ELF/VLF waves generated by "beat-wave" HF heating at high latitudes," *Geophysical Research Letters*, Vol. 41, 4442–4448, 2014.
12. Gavrilov, B. G., Yu I. Zetser, I. A. Ryakhovskii, et al., "Remote sensing of ELF/VLF radiation induced in experiments on artificial modification of the ionosphere," *Geomagnetism and Aeronomy*, Vol. 55, 450–456, 2015.

13. Wait, J. R., "The mode theory of VLF ionospheric propagation for finite ground conductivity," *Proceedings of the IRE*, Vol. 45, 760–767, 1957.
14. Galejs, J., "ELF and VLF fields of a horizontal electric dipole," *IEEE Transactions on Antennas and Propagation*, Vol. 16, 689–700, 1968.
15. Pan, W., *Propagation of Long Wave Very Long Wave and Extremely Long Wave*, University of Electronic Science and Technology Press, Chengdu, 2004.
16. Chang, S., Z. Zhao, and F. Wang, "The downward ELF/VLF waves radiation excited by ionospheric artificial modulation," *Chinese Journal of Geophysics*, Vol. 10, 2458–2467, 2011.
17. Wang, F., "Ray tracing of extremely low frequency waves radiated from ionospheric artificial modulation at low latitude," *Acta Phys Sin*, Vol. 19, 199401–199401, 2012.
18. Huang, W. and S. Gu, "Interaction between the powerful high-frequency radio wave and the lower terrestrial ionosphere," *Chinese Journal of Space Science*, Vol. 3, 181–188, 2003.
19. Li, K. and Y. Miao, "The VLF field of the sea surface generated by the transmitter antenna in the inhomogeneous ionosphere," *Chinese Journal of Radio Science*, Vol. 13, 265–269, 1998.
20. Barr, R. and P. Stubbe, "ELF and VLF radiation from the "polar electrojet antenna"," *Radio Science*, Vol. 19, 1111–1122, 1984.
21. Barr, R. and P. Stubbe, "ELF and VLF wave generation by HF heating: A comparison of AM and CW techniques," *Journal of Atmospheric and Solar-Terrestrial Physics*, Vol. 59, 2265–2279, 1997.
22. Kou, S. P., M. C. Lee, P. Kossey, et al., "Stimulated thermal instability for ELF and VLF wave generation in the polar electrojet," *Geophysical Research Letters*, Vol. 27, 85–88, 2000.
23. Cohen, M. B., R. C. Moore, M. Golkowski, et al., "ELF/VLF wave generation from the beating of two HF ionospheric heating sources," *Journal of Geophysical Research Space Physics*, Vol. 117, 1702–1711, 2012.
24. Chang, S. S., Z. Y. Zhao, and F. Wang, "The downward ELF/VLF waves radiation excited by ionospheric artificial modulation," *Chinese Journal of Geophysics*, Vol. 10, 2458–2467, 2011.